CHIN.PHYS.LETT. Vol. 25, No. 2 (2008) 574

High Speed Signal Wavelength Conversion Using Stimulated Raman Effect in Ultrasmall Silicon-on-Insulator Optical Waveguides *

WU Jian-Wei(吴建伟)[1,2], LUO Feng-Guang(罗风光)[1,2**], GALLEP Cristiano de Mello[3]

[1] *College of Optoelectronics Science and Engineering, Huazhong University of Science and Technology, Wuhan 430074*
[2] *Wuhan National Laboratory for Optoelectronics, Wuhan 430074*
[3] *Telecommunication Technology Division/CESET, State University of Campinas, Limeira, SP, Brazil*

(Received 1 August 2007)

We propose the high speed signal wavelength conversion based on stimulated Raman effect on silicon waveguides. Simulation results of non-return-to-zero (NRZ) pseudorandom bit sequence (2^7-1 code) at 500-Gb/s rate of conversion in an ultrasmall silicon-on-insulator (SOI) optical waveguide are presented by co-propagating pump optical field. The most attractive issue is that the inverted converted signal can be obtained at the same wavelength as that of primary signal. In addition, the conversion performances, including extinction ratio (ER) and average peak power of conversion signal, depend strongly on the launching pump intensity.

PACS: 42.82.−m, 85.30.De, 42.65.Re

Silicon photonics is a rapidly growing field that has made significant advances in recent years, in which the gain coefficient for stimulated Raman scattering (SRS) in silicon is approximately 10^4 times higher than that in silica so that the Raman amplification and laser become possible in silicon waveguide.[1−5] However, nonlinear loss due to the indirect band gap structure, including two-photon absorption (TPA) and free-carrier absorption (FCA) induced by TPA, are limiting factors for optical communication applications. To overcome the nonlinear loss induced by carriers, some approaches such as the reverse biased p-i-n junction, pulsed pumping and scaling down of waveguide dimension, and so on, have been reported, with success in decreasing the carrier lifetime.[6−8]

All optical communication networks will, in a not so distant future, be very dynamic in traffic management, relocating data transfer over the available physical and spectral pathways, enabling as deep as possible a better utilization of the installed network and with minimum hardware, i.e., high costs. The cheapest and most matured semiconductor technology is surely related to silicon and related procedures. Silicon photonics is being used to implement lasers, detectors, ring resonators and very good waveguides. Among the many interesting features of Si-based photonics, wavelength conversion is one of the nonlinear applications of great interest. Up to date, many wavelength conversion devices have been investigated, some based on cross-gain modulation (XGM), cross-phase modulation (XPM) and four-wave mixing (FWM) in nonlinear devices such as semiconductor optical amplifiers (SOA) and special optical fibres where the bit rates and conversion speed are limited by long carrier recovery time and dispersion in these projects and devices.[9−12]

In this way, Si-photonics is the most suitable approach for integrated high speed all optical signal conversion to be suitable for the development of high capacity all optical networks because the dispersion may be neglected for picosecond pulse ($\geq$ 1 ps) and the nonlinear loss is also small for low initial energy in ultrasmall SOI waveguide.[13] The published reports focus on the conversion between different wavelengths using four-wave mixing (FWM) in SOI.[14−16] However, the wavelength conversion may also convert information to the same wavelength, which is very important for applications in WDM switching blocks.[17] A novel project based on the highly integrated ultrasmall SOI optical waveguide has been proposed, to our best knowledge, in which the high speed signal inverted wavelength conversion can be performed between two same wavelengths at 500-Gb/s by using SRS effect. In the presented simulations, the extinction ratio (ER) and power of conversion signal are observed with variational initial peak power of pump wave at different waveguide lengths. In investigation, the FWM process is neglected, which is deeply suppressed due to the large wavevector mismatch in ultrasmall SOI optical waveguide.[18]

In Fig. 1, the rib waveguide structure with width w, rib height H, and slab height h, the central wavelengths of primary signal wave λ_s, λ_p and λ_c are the wavelengths of pump and probe continuous waves (CWs), respectively. Here λ_s and λ_c have the same wavelengths. To obtain higher SRS gain and high quality wavelength conversion, the wavelengths will be selected accurately according to Raman gain peak

*Supported by the National Science Foundation of China under Grant No 60677023 and the National High technology Research and Development Program of China under Grant No 2006AA01Z240.

**To whom correspondence should be addressed. Email: fgluo@mail.hust.edu.cn

© 2008 Chinese Physical Society and IOP Publishing Ltd

frequency shift of 15.6 THz in the silicon waveguide. Therefore, λ_s and λ_c should locate near the Raman gain spectrum peak of λ_p.

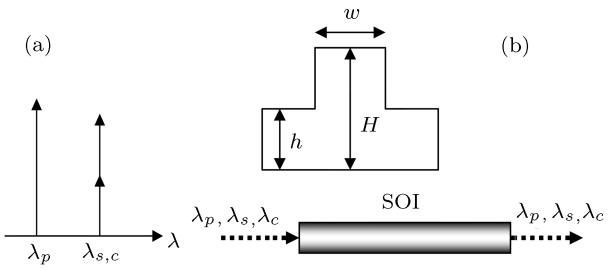


Fig. 1. Schematic diagram of inverted wavelength conversion between two same wavelengths based on SOI.

In the present study, the modified propagation equations of three optical waves can be given by[19]

$$\begin{aligned}
&\frac{\partial A_p}{\partial z}+i\frac{1}{2}\beta_{p2}\frac{\partial^2 A_p}{\partial T^2}\\
&=-\frac{1}{2}\alpha_p A_p-\frac{1}{2}\alpha_{\mathrm{FCA}}A_p-\frac{1}{2}\beta_{\mathrm{TPA}}g_{p,p}|A_p|^2A_P\\
&\quad-\frac{1}{2}\beta_{\mathrm{TPA}}g_{p,s}(|A_s|^2+|A_c|^2)A_p+i\gamma_{p.p}|A_p|^2A_p\\
&\quad+i2\gamma_{p,s}(|A_s|^2+|A_c|^2)A_p+i\frac{\omega_p}{c}\Delta n_pA_p\\
&\quad-\frac{1}{2}g_R\frac{\omega_p}{\omega_s}g_{p,s}(|A_s|^2+|A_c|^2)A_p, \qquad (1)\\
&\frac{\partial A_s}{\partial z}+d\frac{\partial A_s}{\partial T}+i\frac{1}{2}\beta_{s2}\frac{\partial^2 A_s}{\partial T^2}\\
&=-\frac{1}{2}\alpha_s A_s-\frac{1}{2}\alpha_{\mathrm{FCA}}A_s-\frac{1}{2}\beta_{\mathrm{TPA}}g_{p,s}|A_p|^2A_s\\
&\quad-\frac{1}{2}\beta_{\mathrm{TPA}}g_{s,s}(|A_s|^2+|A_c|^2)A_s+i\gamma_{s,s}|A_s|^2A_s\\
&\quad+i2\gamma_{s,s}|A_c|^2A_s+i2\gamma_{p,s}(|A_p|^2)A_s+i\frac{\omega_s}{c}\Delta n_sA_s\\
&\quad+\frac{1}{2}g_Rg_{p,s}(|A_p|^2)A_s, \qquad (2)\\
&\frac{\partial A_c}{\partial z}+d\frac{\partial A_c}{\partial T}+i\frac{1}{2}\beta_{c2}\frac{\partial^2 A_c}{\partial T^2}\\
&=-\frac{1}{2}\alpha_c A_c-\frac{1}{2}\alpha_{\mathrm{FCA}}A_c-\frac{1}{2}\beta_{\mathrm{TPA}}g_{p.s}|A_p|^2A_c\\
&\quad-\frac{1}{2}\beta_{\mathrm{TPA}}g_{s,s}(|A_s|^2+|A_c|^2)A_c+i\gamma_{s,s}|A_c|^2A_c\\
&\quad+i2\gamma_{s,s}|A_s|^2A_c+i2\gamma_{p,s}(|A_p|^2A_c\\
&\quad+i\frac{\omega_c}{c}\Delta n_cA_c+\frac{1}{2}g_Rg_{p,s}(|A_p|^2)A_c, \qquad (3)
\end{aligned}$$

where subscripts p, s and c denote the pump, primary signal and probe optical fields, respectively; A is the slowly varying amplitude, z is the propagation distance; T is the retarded time, $d=\dfrac{1}{v_{gp}}-\dfrac{1}{v_{gs}}$ is the walkoff parameter, with $1/v_{gp}=1.3695\times10^{-8}\,\mathrm{sm}^{-1}$ at $\lambda_p=1550\,\mathrm{nm}$ and $1/v_{gs}=1.3737\times10^{-8}\,\mathrm{sm}^{-1}$ at $\lambda_s=1670\,\mathrm{nm}$; β_2 is the group velocity; λ and ω are the central wavelength and angle frequency of pulses, respectively; α_p is the propagation loss parameter; β_{TPA} is the two-photon absorption parameter; g_R is the Raman gain peak value of pump optical field; α_{FCA}, Δ_n, and $g_{a,b}$ indicate respectively the FCA parameter, the change of effective index due to the free-carrier dispersion (FCD), and the overlap integral, and can be given by[19,20]

$$\begin{aligned}
\alpha_{\mathrm{FCA}}&=8.5\times10^{-18}\Big(\frac{\lambda}{1.55}\Big)^2\Delta n_e\\
&\quad+6.0\times10^{-18}\cdot\Big(\frac{\lambda}{1.55}\Big)^2\Delta n_h\\
&=\sigma\cdot n=\sigma_0\Big(\frac{\lambda}{1.55}\Big)^2 n, \qquad (4)\\
\Delta n&=-8.8\times10^{-22}\cdot\Big(\frac{\lambda}{1.55}\Big)^2\Delta n_e\\
&\quad-8.5\times10^{-18}\Big(\frac{\lambda}{1.55}\Big)^2(\Delta n_h)^{0.8}, \qquad (5)\\
g_{a,b}&=\frac{\int\int|F_a(x,y)|^2|F_b(x,y)|^2dxdy}{\int\int|F_a(x,y)|^2dxdy\int\int|F_b(x,y)|^2dxdy},\\
&\quad a,b=p,s, \qquad (6)
\end{aligned}$$

where $n=n_e=n_h$ is the density of electron-hole pairs generated by the TPA process. The coefficient $\sigma_0=1.45\times10^{-17}\,\mathrm{cm}^2$[21] is the FCA cross section measured at $\lambda=1550\,\mathrm{nm}$, $F(x,y)$ is the optical mode distribution in the waveguide cross-section.

In Eqs. (1) and (3), the coefficients $\gamma_{a,a}(a=p,s)$ and $\gamma_{a,b}$ $(a,b=p$ or $s)$ denote the self-phase and cross-phase modulations parameters, and are described by

$$\gamma_{a,a}=\frac{\omega_{p,s}}{2cn_{\mathrm{eff}}}g_{a,a}(\chi^{NR}_{xxxx}+\chi^R(0)), \qquad (7)$$

$$\gamma_{a,b}=\frac{\omega_{p,s}}{2cn_{\mathrm{eff}}}g_{a,b}(\chi^{NR}_{xxyy}), \qquad (8)$$

where n_{eff} is the effective index; $\chi^{NR}_{xxxx}(=0.5\times10^{-18}\,\mathrm{m}^2\mathrm{V}^{-2}=2\chi^{NR}_{xxyy}$ [22]) is the electronic nonresonant susceptibility; χ^R the Raman resonant susceptibility can be written as

$$\chi^R(\omega_s,\omega_p-\omega_s,\omega_s)=\frac{2\Omega_R\Gamma_R\xi_R}{2i\Gamma_R\Delta\omega+\Omega_R^2-\Delta\omega^2}, \qquad (9)$$

where $\Omega_R(=15.6\,\mathrm{THz})$ is the Raman frequency shift, $\xi_R(=11.2\times10^{-18}\,\mathrm{m}^2\mathrm{V}^{-2})$ is the Raman susceptibility when $\Delta\omega=\Omega_R$, $\Gamma_R(=2\pi\times53\,\mathrm{GHz})$ is the resonance half-width.[22]

To obtain a consistent mathematical model, Eqs. (1) and (3) have been coupled to the rate equation governing the free carrier dynamic into the waveguide, given by[23]

$$\begin{aligned}
\frac{dn}{dT}&=-\frac{n}{\tau_{\mathrm{eff}}}+\frac{\beta_{\mathrm{TPA}}}{2\hbar\omega_p}(|A_p(z,T)|^2g_{p,p})^2\\
&\quad+\frac{\beta_{\mathrm{TPA}}}{2\hbar\omega_s}[(|A_s(z,T)|^2+|A_c(z,T)|^2)g_{s,s}]^2, \qquad (10)
\end{aligned}$$

where n is the carriers density, $\hbar$ is the reduced Planck constant, and τ_{eff} is the relevant effective recombination lifetime for free carrier, denoted by[24]

$$\tau_{\text{eff}}^{-1} = \frac{S}{H} + \frac{w + 2(H-h)}{wH} S' + 2\frac{h}{H}\sqrt{\frac{D}{w^2}\Big(\frac{S+S'}{h}\Big)}, \tag{11}$$

where the first term refers to the interface recombination lifetime, the second term refers to the surface recombination at the sidewalls, and the last term refers to transit time out of the modal area. S and S' are the effective surface recombination velocity, D is the diffusion coefficient.

It is worth noting that higher order Stokes waves have not been considered because the maximum of fundamental order Stokes wave is further lower than Raman threshold power in our modelling. In the following, we present the simulation results.

According to Refs. [24-26], we list all the parameters for simulation in Table 1.

Table 1. Simulation parameters.

Parameter	Definition	Value
$\alpha_{p,s,c}$	Waveguide linear loss coefficient	$0.22\,\text{dB cm}^{-1}$
g_R	Raman gain at 1670 nm	59×10^{-9} cm W^{-1}
β_{TPA}	Two-photon absorption coefficient	$0.5\,\text{cm GW}^{-1}$
β_{p2}	Group velocity dispersion at λ_p	$-0.2\,\text{ps}^2\text{m}^{-1}$
$\beta_{s,c2}$	Group velocity dispersion at $\lambda_{s,c}$	$-0.4\,\text{ps}^2\text{m}^{-1}$
w	Rib waveguide width	900 nm
H	Rib height	780 nm
h	Slab height	390 nm
S, S'	Effective surface recombination velocity	$80\,\text{ms}^{-1}$
D	Diffusion coefficient	$16\,\text{cm}^2\text{s}^{-1}$
c	Light velocity in vacuum	$2.99792458 \times 10^8\,\text{ms}^{-1}$
$\hbar$	Reduced Planck constant	1.06×10^{-34} Js
λ_s	Primary signal wavelength	1670 nm
λ_c	Probe wavelength	1670 nm
λ_p	Pump wavelength	1550 nm

Figure 2 shows the time domain waveforms of initial primary signal [Fig. 2(a)] and output conversion signal pulses [Fig. 2(b)] at 500 Gb/s. It is shown that the conversion signal is inverted as compared with the primary signal after going through the SOI waveguide. However, the bit rate is so high that the situation changes dramatically because carriers produced by previous pulse have not enough time to recombine before the next pulse arrives. Thus, the density of carriers from pulse to pulse increases until a steady state is reached. In numerical simulations, the steady state waveform is shown in Fig. 2(b) by propagating enough pulses. The principle of wavelength conversion can be explained such that the primary signal will obtain the energy from the pump optical field due to SRS, i.e., the energy of pump wave will be transferred to the primary signal in which the transfer efficiency is proportional with the overlapped energy between two optical fields. Therefore, the pump optical field will be modulated by the primary signal owing to SRS process so that it has inverted waveform compared to the primary signal shape. Simultaneously, the modulated pump optical field will also act on the cw probe optical field by SRS leading to energy transfer from modulated pump wave to the cw probe, namely the exchange of information between primary signal and probe wave channels can be indirectly carried out by the pump wave. Finally, the inverted conversion signal is generated with the centre wavelength of 1670 nm at the output end of SOI waveguide.

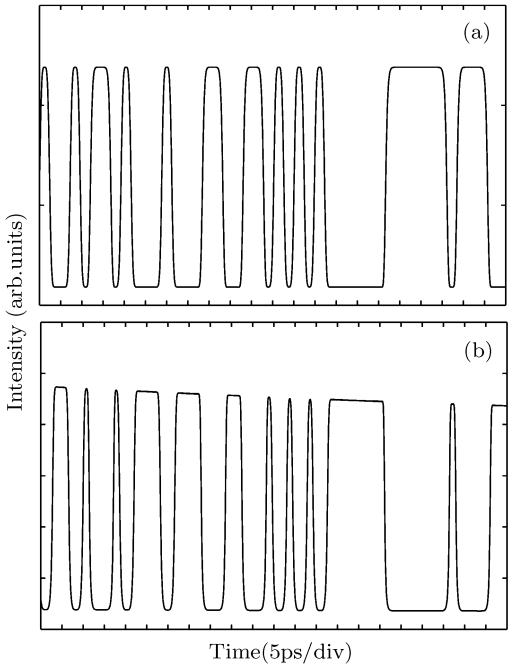


Fig. 2. Intensity envelopes of initial primary signal and output inverted conversion signal with initial peak power 34.77 dBm, 6.99 dBm, and −13.01 dBm for optical field λ_p, λ_s, and λ_c, respectively, and waveguide length $L = 6$ mm, and the ER of 16.68 dB for primary signal.

In fact, the qualities of wavelength conversion signal are strongly dependent on the incident powers of the three optical fields as well as waveguide length. The power of primary signal, however, is low after passing through a long distance, which is fixed at 0 dBm in our simulation. The power of initial probe wave is set to −13.01 dBm at the input of the waveguide because the lower probe power is beneficial for improving the ER of conversion signal that is a very important parameter for evaluating the performance of wavelength conversion, and defined by

$$\text{ER} = 10\log\frac{\text{bit}_1^{\min}}{\text{bit}_0^{\max}}, \tag{12}$$

where ER has the unit of dB, $\text{bit}_1^{\min}$ and $\text{bit}_0^{\max}$ denote respectively the lower 1-bit level and the higher 0-bit level of conversion signal.

Figures 3 and 4 show the ER and average peak power of conversion signal as a function of initial power of pump at different waveguide lengths, to present the qualities of conversion signal. It is clearly shown that both of them grow sub-linearly as a result of SRS with increase of the input pump peak power, but the slopes of curves will become smaller and smaller due to pump depletion (gain saturation) and losses, i.e., the ER and average peak power may arrive at the maximum with increasing the pump power.

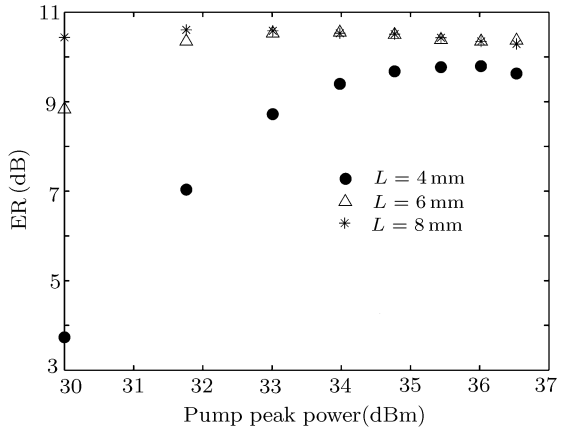


Fig. 3. *ER* versus the initial pump peak power with different waveguide lengths.

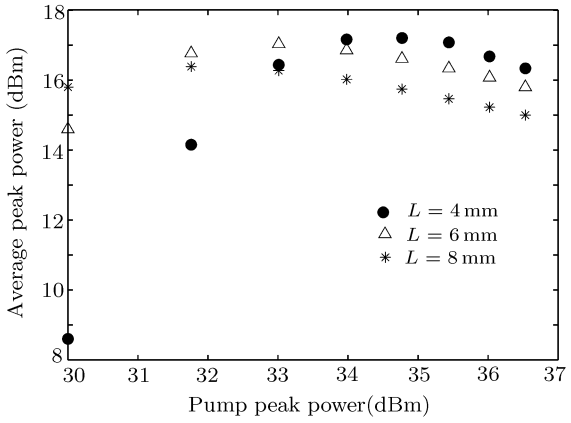


Fig. 4. Average peak power versus the initial peak power with different waveguide lengths.

In addition, one can see that when the pump power is low, the larger ER and average peak power can be achieved for 8-mm-long waveguide compared with shorter waveguides because of longer interaction distance of SRS, which may become smaller than that of the case of shorter waveguide as a result of gain saturation and losses when enhancing further the input pump power.

In summary, we have presented a comprehensive numerical study of high speed signal wavelength conversion between two same wavelengths based on stimulated Raman scattering in ultrasmall silicon-on-insulator optical waveguide. The extinction ratio and average peak power of the inverted conversion signal depend strongly on the length of silicon waveguide and initial peak power of pump optical field. On the basis of the above analysis, we conclude that high quality conversion signal with larger ER and high power can be achieved by adjusting the initial pump peak power and waveguide length.

References

[1] Tsang H K, Wong C S and Liang T K 2002 *Appl. Phys. Lett.* **80** 416
[2] Rieger G W, Virk K S and Young J F 2004 *Appl. Phys. Lett.* **84** 900
[3] Rong H, Jones R, Liu A et al 2005 *Nature* **433** 725
[4] Yin L, Lin Q and Agrawal G P 2006 *Opt. Lett.* **31** 1295
[5] Culurciello E 2007 *Electron. Lett.* **43** 418
[6] Rong H, Liu A, Jones R et al 2005 *Nature* **433** 292
[7] Liu A, Rong H, Paniccia M et al 2004 *Opt. Express* **12** 4261
[8] Espinola R L, Dadap J I, Osgood R M et al 2004 *Opt. Express* **12** 3713
[9] Gallep C M, Cavalcanti A L R, Ribeiro N et al 2006 *Microwave Opt. Technol. Lett.* **48** 1141
[10] Dong J, Fu S, Zhang X et al 2006 *IEEE Photon. Technol. Lett.* **18** 2554
[11] Simos H, Stamataki I, and Syvridis D 2007 *IEEE J. Quantum. Electron.* **43** 370
[12] Andersen P A, Tokle T, Geng Y et al 2005 *IEEE Photon. Technol. Lett.* **17** 1908
[13] Yin L, and Agrawal G P 2007 *Opt. Lett.* **32** 2031
[14] Espinola R L, Dadap J I, Osgood R M et al 2005 *Opt. Express* **13** 4341
[15] Kuo Y, Rong H, Sih V et al 2006 *Opt. Express* **14** 11721
[16] Yamada K, Fukuda H, Tsuchizawa T et al 2006 *IEEE Photon. Technol. Lett.* **18** 1046
[17] Liu Y, Hill M T, Tangdiongga E et al 2003 *IEEE Photon. Technol. Lett.* **15** 90
[18] Jalali B, Claps R, Dimitropoulos D et al 2004 *Topics Appl. Phys.* **94** 199
[19] Passaro V M N, Leonardis F D 2006 *Opt. and Quantum Electron.* **38** 877
[20] Soref R A, and Bennett B R 1987 *IEEE Quantum Electron.* **23** 123
[21] Claps R, Rahgunathan V, Dimitropoulos D et al 2004 *Opt. Express* **12** 2774
[22] Dimitropoulos D, Raghunathan V, Claps R et al 2004 *Opt. Express* **12** 149
[23] Liu A, Rong H, Jones R et al 2006 *J. Lightwave Technol.* **24** 1440
[24] Dimitropoulos D, Jhaveri R, Claps R et al 2005 *Appl. Phys. Lett.* **86** 07115-1
[25] Dadap J I, Espinola R L, Osgood R M et al 2004 *Opt. Lett.* **29** 2755
[26] Lin Q, Zhang J, Fauchet P M et al 2006 *Opt. Express* **14** 4786